MATERIALS CHEMISTRY FRONTIERS

RESEARCH ARTICLE

View Article Online
View Journal | View Issue

Cite this: *Mater. Chem. Front.*, 2023, **7**, 4944

Efficient narrow green organic light-emitting diodes with low efficiency roll-offs based on iridium(III) complexes containing indolo[3,2,1-*jk*]carbazole and pyrimidine units†

Qi-Ming Liu,[a] Li Yuan,[a] Xiang-Ji Liao,[a] Xiao-Sheng Zhong,[a] Hua-Xiu Ni,[a] Yu Wang,[a] Yue Zhao *[a] and You-Xuan Zheng *[ab]

In this work, two iridium(III) complexes, **(2-pymICz)$_2$Ir(tmd)** and **(4-pymICz)$_2$Ir(tmd)**, using 2-(pyrimidine-2-yl)indolo[3,2,1-*jk*]carbazole (2-pymICz) and 2-(6-(methyl)pyrimidine-4-yl)indolo[3,2,1-*jk*]carbazole (**4-pymICz**) as the main ligands, which incorporate the rigid indolo[3,2,1-*jk*]carbazole (ICz) unit and 2,2,6,6-tetramethyl-3,5-heptanedione (tmd) as an ancillary ligand were synthesized. The Ir(III) complexes exhibit green photoluminescence (PL) with emission peaks at 515 and 523 nm, and relatively narrow full width at half maximum (FWHM) bands of 53 and 57 nm, and PL quantum yields (PLQYs) of 70% and 73%, respectively, in dichloromethane solutions. When these complexes were doped into the bipolar host 2,6DCzPPy (2,6-bis(3-(9*H*-carbazol-9-yl)phenyl)pyridine), the PLQYs of the resulting films significantly increased to 98.5% and 92.5%, accompanied by narrower FWHMs of 38 and 43 nm. Organic light-emitting diodes (OLEDs) based on these two emitters display good performance characteristics. Notably, the device based on **(2-pymICz)$_2$Ir(tmd)** exhibits better performances with a maximum external quantum efficiency (EQE_{max}) of 31.3%. Even at a high brightness of 10 000 cd m^{-2}, the EQE of this device still can reach 30.4%, indicating an extremely low efficiency roll-off of below 3%. Both devices show narrow electroluminescence FWHMs of 40 and 44 nm, respectively. Overall, the study highlights the practicality of incorporating rigid ICz groups and nitrogen atoms into the main ligands of Ir(III) complexes as a viable strategy for achieving efficient OLEDs with narrow emission spectra, high efficiencies, and low efficiency roll-offs.

Received 4th May 2023,
Accepted 1st August 2023

DOI: 10.1039/d3qm00514c

rsc.li/frontiers-materials

Introduction

Organic light emitting diodes (OLEDs) have garnered significant attention in the display field due to their advantages of self-luminescence, high efficiency, wide viewing angle, ultra-thinness, and flexibility.[1–4] The success of OLEDs relies heavily on the choice of emissive materials used in their construction. Among the several generations of OLED emitters, phosphorescent materials, in particular, have shown promise in harnessing both singlet and triplet excitons for luminescence, theoretically achieving a 100% internal quantum efficiency (IQE).[5,6] Among the phosphorescent emitters, iridium(III) complexes have emerged as commercially desirable OLED materials due to their facile chemical synthesis, tunable photophysical properties, excellent stability, and long device operation lifetime.[7,8] However, most Ir(III) complexes exhibit high efficiencies but broad emission spectra resulting from their complex emission components such as singlet/triplet metal-to-ligand charge transfer (^{1}MLCT and ^{3}MLCT) and triplet ligand-to-ligand charge transfer (^{3}LLCT).[9] This broad emission spectrum necessitates the use of color filters in commercial OLED displays to selectively filter out specific wavelengths of light, leading to energy loss and reduced device efficiency. Therefore, there is a need to develop efficient Ir(III) complexes with narrow full width at half maximum (FWHM) bands to meet the demands of commercial OLED displays.

To achieve narrow bandwidth in Ir(III) complexes, one effective strategy is to incorporate rigid units into the ligands, thereby restricting the free relaxation of the complexes.[10] Among the available rigid groups, indolo[3,2,1-*jk*]carbazole (ICz) stands out as a planar and rigid aromatic unit with excellent thermal and morphological stability,[11] high carrier-transport ability,[12] and high triplet excitation energy,[13] which has been widely used in

[a] *State Key Laboratory of Coordination Chemistry, Jiangsu Key Laboratory of Advanced Organic Materials, School of Chemistry and Chemical Engineering, Nanjing University, Nanjing 210093, P. R. China. E-mail: yxzheng@nju.edu.cn*
[b] *Shenzhen Research Institute of Nanjing University, Shenzhen 518057, P. R. China*

† Electronic supplementary information (ESI) available. CCDC 2259293. For ESI and crystallographic data in CIF or other electronic format see DOI: https://doi.org/10.1039/d3qm00514c

materials for solar cells[14] and OLEDs.[15] In our previous work, we successfully incorporated the ICz unit into Ir(III) complexes for the first time, and the OLED based on a green emitter $(pyidcz)_2Ir(tmd)$ (pyidcz: 2-(pyridin-2-yl)indolo[3,2,1-*jk*]carbazole, tmd: 2,2,6,6-tetramethyl-3,5-heptanedione) exhibited a maximum external quantum efficiency (EQE_{max}) of 21.2%, and an electroluminescence (EL) spectrum peaking at 502 nm with a FWHM of 33 nm.[10] Similarly, the OLED based on an Ir(III) complex containing a pyrido[3′,2′:4,5]pyrrolo[3,2,1-*jk*]carbazole unit showed an EQE_{max} of 23.8%, and an EL spectrum peaking at 501 nm with a narrow FWHM as low as 30 nm and a maximum external quantum efficiency (EQE_{max}) of 23.8%.[16] These results demonstrate the promise for incorporating rigid ICz units into the main ligand of Ir(III) complexes for the development of efficient emitters and their OLEDs with narrow emissions.

Generally, the hole transport ability of most hole transporting materials in OLEDs is higher than the electron transport ability of electron transporting materials. To balance the carrier injection and transport in the emissive layer, introduction of electron transporting groups into the ligand is an effective approach to improve the electron mobility of the entire complex.[17–21] This strategy has been successfully demonstrated in several studies by introducing electron transporting groups into the main ligands of Ir(III) complexes, resulting in improved device efficiency and reduced efficiency roll-off.[22–26]

In the light of the above consideration, two novel green Ir(III) complexes were synthesized featuring bipolar main ligands, 2-(pyrimidine-2-yl)indolo[3,2,1-*jk*]carbazole (2-pymICz) and 2-(6-(methyl)pyrimidine-4-yl)indolo[3,2,1-*jk*]carbazole (**4-pymICz**), which consisted of electron-rich ICz and electron-deficient pyrimidine moieties, thereby achieving a balanced injection of charge carriers.[27] tmd was selected as an ancillary ligand due to its minimal interference with the photophysical properties of the Ir(III) complexes, as well as its ability to reduce self-quenching and efficiency roll-off in OLEDs.[7,28] The synthesized **$(2\text{-pymICz})_2Ir(tmd)$** and **$(4\text{-pymICz})_2Ir(tmd)$** complexes show high PL quantum yields (PLQYs) exceeding 90% in doped films. Furthermore, both complexes demonstrate short phosphorescence lifetimes (τ) of approximately 0.2 and 1 μs in solution and doped films, respectively. The resulting OLEDs exhibit good performances with narrow FWHMs of less than 45 nm, and high EQE_{max} values of up to 31.3% with extremely low efficiency roll-off.

Experimental section

Scheme 1 illustrates the synthetic routes for the ligands and complexes. Compounds **1–4** were synthesized following the methods described in our previously published work.[10] All reagents utilized in the synthetic procedures were commercially purchased and used as received without further purification. The reactions were conducted under an inert gas atmosphere using standard Schlenk techniques. The molecular structures of resulting Ir(III) complexes were characterized by ^1H NMR, ^{13}C NMR (Fig. S1–S7, ESI†) and high resolution mass spectroscopy (HRMS, Fig. S8 and S9, ESI†).

Synthesis of the main ligands 2-pymICz and 4-pymICz

Compound **4** (2.5 mmol), 2-chloroprimidine (3 mmol) or 4-chloro-6-methylpyrimidine (3 mmol), $Pd(dppf)Cl_2$ (0.125 mmol)

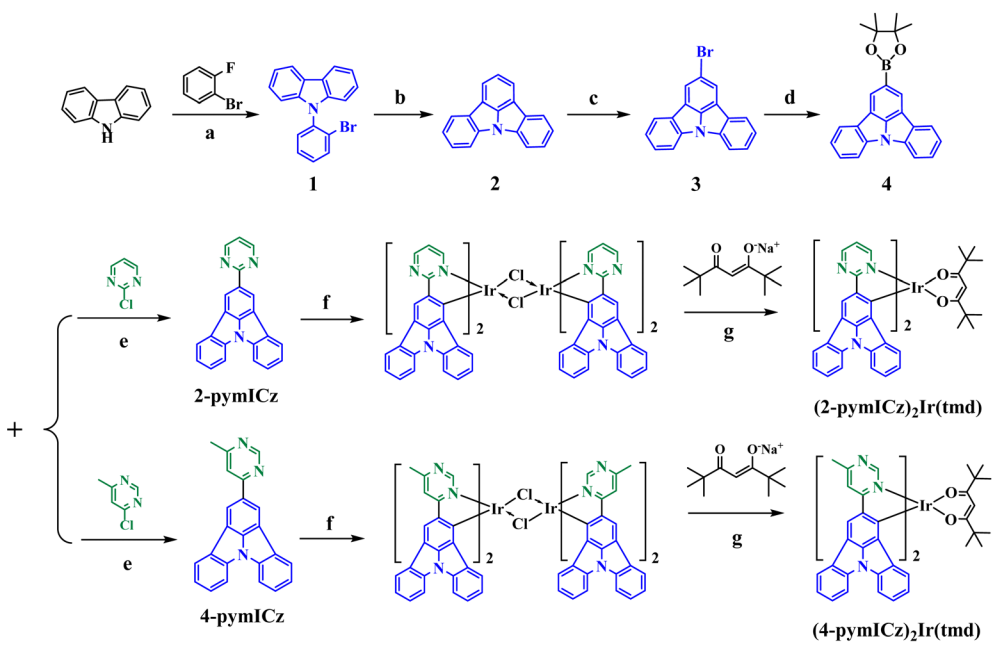

(a): ^{t}BuOK, DMF, 150 °C, 12 h; (b): $Pd(OAc)_2$, K_2CO_3, DMAC, 170 °C, 12 h; (c): NBS, DCM, r.t., 12 h; (d): $Pd(dppf)Cl_2$, KOAc, Dioxane, 100 °C, 12h;
(e): $Pd(dppf)Cl_2$, Cs_2CO_3, Dioxane/H_2O, 12 h; (f): $EtOCH_2CH_2OH/H_2O$, 110 °C, 12 h; (g): $EtOCH_2CH_2OH$, 110 °C, 12 h

Scheme 1 Synthesis routes of the ligands and Ir(III) complexes.

and Cs_2CO_3 (7.5 mmol) were dissolved in a mixed solution of dioxane (20 mL) and water (2 mL), and the solution was refluxed at 100 °C overnight under a nitrogen atmosphere. Then the solvent was removed by vacuum distillation, and the residues were purified by silica gel column chromatography (petroleum ether (PE)/ether (EA) = 3 : 1 (v/v)).

2-pymICz (white solid, 66.4% yield): ^{1}H NMR (400 MHz, chloroform-d) δ 9.26 (s, 2H), 8.89 (d, J = 4.8 Hz, 2H), 8.20 (d, J = 7.7 Hz, 2H), 7.91 (d, J = 8.0 Hz, 2H), 7.58 (td, J = 7.8, 1.2 Hz, 2H), 7.39 (td, J = 7.7, 1.0 Hz, 2H), 7.22 (t, J = 4.7 Hz, 1H).

4-pymICz (white solid, 72.0% yield): ^{1}H NMR (400 MHz, chloroform-d) δ 9.20 (d, J = 1.3 Hz, 1H), 8.82 (s, 2H), 8.19 (dt, J = 7.8, 1.0 Hz, 2H), 7.93 (dt, J = 8.1, 0.9 Hz, 2H), 7.83 (d, J = 1.4 Hz, 1H), 7.61 (ddd, J = 8.2, 7.4, 1.2 Hz, 2H), 7.41 (td, J = 7.6, 1.0 Hz, 2H), 2.69 (s, 3H).

Synthesis of Ir(III) complexes

To synthesize the Ir(III) complexes, **2-pymICz** or **4-pymICz** main ligand (2.2 mmol) and $IrCl_3$ (1 mmol) were dissolved in a mixed solution of ethylene glycol diethyl ether (20 mL) and water (5 mL), and the resulting mixture was refluxed at 110 °C overnight under N_2 protection. After cooling to room temperature, water was added into the solution, and the precipitated yellow powders of corresponding chloride-bridged dimer were obtained by filtering, washing and drying in sequence.

The resulting chlorine-bridge dimer (0.2 mmol) and tma-Na (0.8 mmol) were then dissolved in ethylene glycol diethyl ether (20 mL), and the solution was refluxed at 110 °C overnight under a nitrogen atmosphere. Finally, the solvent was removed by vacuum distillation, and the residues were purified by silica gel column chromatography (dichloromethane (DCM)/PE = 1/1 (v/v)).

(2-pymICz)$_2$Ir(tmd) (yellow solid, 31.3% yield): ^{1}H NMR (400 MHz, chloroform-d) δ 9.22 (s, 2H), 8.87 (dd, J = 4.7, 2.3 Hz, 2H), 8.25 (dd, J = 5.7, 2.2 Hz, 2H), 8.18 (dd, J = 7.9, 1.2 Hz, 2H), 7.78 (d, J = 7.9 Hz, 2H), 7.68 (d, J = 7.9 Hz, 2H), 7.46 (d, J = 1.3 Hz, 2H), 7.33 (d, J = 1.1 Hz, 2H), 7.17 (d, J = 1.3 Hz, 2H), 6.84 (dd, J = 5.7, 4.6 Hz, 2H), 6.67 (d, J = 1.0 Hz, 2H), 6.43 (d, J = 7.9 Hz, 2H), 5.40 (s, 1H), 0.82 (s, 18H). HR-MS (ESI†) m/z: calculated for $C_{55}H_{43}IrN_6O_2$ $[M + H]^+$, 1013.3150; observed $[M + H]^+$, 1013.3147.

(4-pymICz)$_2$Ir(tmd) (yellow solid, 41.6% yield): ^{1}H NMR (400 MHz, chloroform-d) δ 8.81 (s, 2H), 8.49 (s, 2H), 8.16 (d, J = 7.8 Hz, 2H), 8.11 (s, 2H), 7.80 (d, J = 7.9 Hz, 2H), 7.68 (d, J = 7.9 Hz, 2H), 7.50–7.45 (m, 2H), 7.36 (d, J = 7.7 Hz, 2H), 7.21–7.16 (m, 2H), 6.63 (d, J = 7.6 Hz, 2H), 6.52 (d, J = 7.9 Hz, 2H), 5.43 (s, 1H), 2.82 (s, 6H), 0.81 (s, 18H). HR-MS (ESI†) m/z: calculated for $C_{57}H_{47}IrN_6O_2$ $[M + H]^+$, 1041.3463; observed $[M + H]^+$, 1041.3465.

Results and discussion

Synthesis and characterization

Scheme 1 outlines the synthesis routes employed for the synthesis of the main ligands and Ir(III) complexes. The main ligands were synthesized *via* a five-step synthetic pathway starting from commercially available starting materials. To obtain the Ir(III) complexes **(2-pymICz)$_2$Ir(tmd)** and **(4-pymICz)$_2$Ir(tmd)**, the dichloro-bridged dimers were initially synthesized and subsequently reacted with the ancillary ligand tmd. Evaluated by thermogravimetric analysis (TGA) curves (Fig. S10, ESI†), the decomposition temperatures (T_d, 5% loss of weight) of the two Ir(III) complexes were found to be 264 and 227 °C, respectively, indicating their suitability for the OLED fabrication.

The single crystal of **(2-pymICz)$_2$Ir(tmd)** was grown through slow solvent diffusion of petroleum ether into dichloromethane solution at room temperature. The molecular structure of **(2-pymICz)$_2$Ir(tmd)** was characterized using X-ray crystallography. The single-crystal diagram is depicted in Fig. 1, and the corresponding crystallographic data are provided in Tables S1 and S2 (ESI†). As shown in Fig. 1, the iridium center is coordinated with two C^N main ligands and one O^O ancillary ligand, resulting in a distorted octahedral coordination geometry. The dihedral angle of C–Ir–N is approximately 80°, while the dihedral angle of O–Ir–O is 87.54°. The Ir–C bond lengths are 1.983 and 1.998 Å, slightly shorter than the Ir–N bond lengths of 2.021 and 2.023 Å. The Ir–O bond lengths are approximately 2.1 Å, consistent with the reported Ir–O bond lengths for similar Ir–tmd structures.[29] The crystal structure analysis provides valuable insights into the coordination environment of the complex, which can influence the photophysical and electrochemical properties of the complex.

Photophysical properties

The ultraviolet-visible absorption (UV-Vis) and PL spectra of the Ir(III) complexes were measured in DCM at the room temperature, as shown in Fig. 2. The absorption spectra show intense absorption below 300 nm, which can be attributed to the spin-allowed ligand-to-ligand charge transfer (^{1}LLCT) and ligand-centered (^{1}LC)

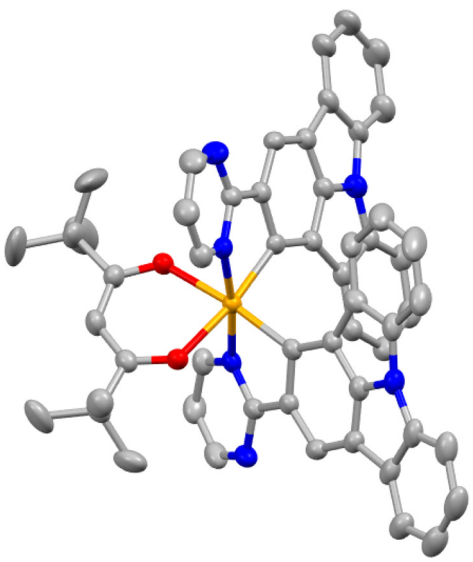

Fig. 1 The single crystal diagram of **(2-pymICz)$_2$Ir(tmd)** (CCDC: 2259293) drawn by Mercury. Hydrogen atoms are omitted for clarity. Ellipsoids are drawn at the 50% probability level.

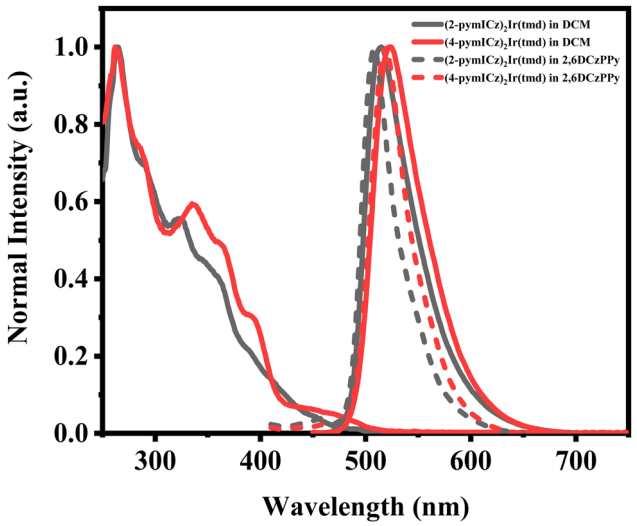

Fig. 2 Normalized UV-Vis and PL spectra (in solutions and doped films) of Ir(III) complexes at room temperature.

transitions of cyclometalated and ancillary ligands while the weaker absorption bands observed at longer wavelengths between 300 and 500 nm can be assigned to spin-allowed ^{1}MLCT, spin-forbidden ^{3}MLCT and ligand-centered (^{3}LC) transitions, which arise *via* the strong spin–orbital coupling (SOC) effect of the transition metal iridium.[30] It is worth noting that although these triplet absorption bands are not as distinct as the singlet transitions, they still significantly contribute to the overall absorptivity of the complexes.[31]

The PL spectra of the two Ir(III) complexes were analyzed to understand their emission properties. The emission spectra show green color emission with maximum wavelengths of 515 and 523 nm for **(2-pymICz)$_2$Ir(tmd)** and **(4-pymICz)$_2$Ir(tmd)**, respectively, which could be attributed to the structural differences in the main ligands. The observed bathochromic shift of 8 nm in **(4-pymICz)$_2$Ir(tmd)** compared to **(2-pymICz)$_2$Ir(tmd)** was in agreement with the smaller energy gaps (E_g) calculated by electrochemical measurements. Additionally, the PL spectra measured in the doped films in the widely used bipolar host material 2,6DCzPPy (2,6-bis(3-(9*H*-carbazol-9-yl)phenyl)pyridine) show a slight hypsochromic shift compared to the spectra obtained in DCM solutions, with FWHMs of 38 and 43 nm. Furthermore, the PL spectra of the complexes measured at 77 K in DCM (Fig. S11, ESI†) exhibit narrower FWHMs as 35 and 41 nm due to the reduced vibrational relaxation in the frozen medium.

The PLQYs of the two Ir(III) complexes were measured to be 70.3% and 72.9% in deoxygenated DCM, respectively (Table 1 and Fig. S12, ESI†). However, when the complexes were doped into the host material 2,6DCzPPy, the PLQYs increased significantly to 98.5% and 92.5% for **(2-pymICz)$_2$Ir(tmd)** and **(4-pymICz)$_2$Ir(tmd)** complexes, respectively (Fig. S14, ESI†). The narrower full width at half maximum (FWHM) bandwidths and higher PLQYs observed in the doped films compared to the complexes in solution can be attributed to the orientational molecular arrangement in the doped films, which reduces vibrational relaxation and enhances photon transport efficiency. Furthermore, compared with our previous reported (pyidcz)$_2$-Ir(tmd) complex containing ICz and pyridine units, the FWHMs of **(2-pymICz)$_2$Ir(tmd)** and **(4-pymICz)$_2$Ir(tmd)** are broader. This can be attributed to the addition of a nitrogen atom in the main ligands, which introduces increased stretching and bending vibrations, resulting in broadened emission spectra.

In addition to the spectral characteristics, the short excited state lifetimes of dopants play a crucial role in reducing the triplet–triplet annihilation (TTA) and triplet–polaron annihilation (TPA) effects in the emissive layer of OLED devices,[32–34] which can lead to low device efficiency roll-off. In this work, the lifetimes of the complexes are in the range of microseconds, specifically, 0.20 and 0.29 μs in solutions (Fig. S13, ESI†), 1.10 and 0.90 μs in doped films (Fig. S15, ESI†). The short lifetimes and high PLQYs of the doped films indicate the potential of these complexes for OLED applications.

Electrochemical properties and theoretical calculations

The frontier molecular orbitals, specifically the highest occupied molecular orbital (HOMO) and lowest unoccupied molecular orbital (LUMO), play a crucial role in determining the color and efficiency of photoelectric materials. Furthermore, the accurate determination of HOMO and LUMO energy levels is crucial for the design of device structures, as it provides insights into the energy level alignment and charge transport mechanisms in the material.

To measure the actual HOMO/LUMO energy levels of **(2-pymICz)$_2$Ir(tmd)** and **(4-pymICz)$_2$Ir(tmd)**, cyclic voltammetry (CV) measurements were conducted in deoxygenated CH_3CN with ferrocene as the standard substance (Fig. S16, ESI†). The HOMO energy levels for **(2-pymICz)$_2$Ir(tmd)** and **(4-pymICz)$_2$Ir(tmd)** complexes were calculated to be −5.39 and −5.37 eV, respectively, using the equation of $E_{HOMO} = -[E_{OX} - E_{(Fc/Fc^+)} + 4.8]$ eV.[35] Furthermore, the LUMO energy levels of **(2-pymICz)$_2$Ir(tmd)** and **(4-pymICz)$_2$Ir(tmd)** complexes were calculated to be −2.99 and −3.00 eV, respectively, combining with the band gaps calculated from the onset of UV-Vis spectra with the equation of $E_{LUMO} = E_{HOMO} + E_g$.

To gain further insight into the electronic structure and excited states of the **(2-pymICz)$_2$Ir(tmd)** and **(4-pymICz)$_2$Ir(tmd)**

Table 1 Photophysical data of Ir(III) complexes

Complex	T_d[a] (°C)	λ_{abs}[b] (nm)	λ_{em}[c] (nm)	FWHM[c] (nm)	$\tau_{298\,K}$[c] (μs)	Φ_{PL}[c] (%)	E_g[d] (eV)	HOMO/LUMO[e] (eV)
(2-pymICz)$_2$Ir(tmd)	264	321/390	515/509	53/38	0.20/1.10	70.3/98.5	2.40	−5.39/−2.99
(4-pymICz)$_2$Ir(tmd)	227	337/392	523/518	57/43	0.29/0.90	72.9/92.5	2.37	−5.37/−3.00

[a] Decomposition temperature calculated from TGA curves. [b] Measured in DCM at 298 K. [c] Measured in DCM in a N_2 atmosphere and doped films in 2,6DCzPPy. [d] Calculated from the onset of the UV-Vis spectrum. [e] Calculated from cyclic voltammetry analysis.

complexes, theoretical calculations were performed. Time-dependent density functional theory (TD-DFT) was employed to calculate the frontier molecular orbitals of the complexes, with a specific LanL2DZ basis set for the center iridium atom and a B3LYP (6-31G) method with GenECP basis for other atoms.[36] The calculated HOMO/LUMO electron cloud distribution patterns and compositions of each fragment were illustrated in Fig. S17 (ESI†). The results demonstrated the ancillary ligand, tmd, has a negligible contribution to the HOMO/LUMO distributions, while the main ligands play the most significant role. Respectively, the HOMO electron cloud distributions of **(2-pymICz)$_2$Ir(tmd)** and **(4-pymICz)$_2$Ir(tmd)** are mainly distributed in the main ligands (72.12% and 67.53%) and iridium atom (24.90% and 28.09%), while the LUMO electron cloud distributions are basically distributed in the main ligands (93.16% and 95.32%). Therefore, it can be concluded the photophysical properties of the Ir(III) complexes are mainly determined by the organometallic main ligands. The energy gaps (E_gs) between HOMO and LUMO of both complexes were calculated to be 3.52 eV, while the HOMO and LUMO energy levels of **(4-pymICz)$_2$Ir(tmd)** are slightly lower than those of **(2-pymICz)$_2$Ir(tmd)**. This observation may be attributed to the different positions of the nitrogen atom on the pyrimidine group, which can influence the electronic structure and energy levels of the complexes.

Furthermore, the interfragment charge transfer (IFCT) method was used to gain insight into the charge transfer mechanism in excited states of **(2-pymICz)$_2$Ir(tmd)** and **(4-pymICz)$_2$Ir(tmd)** complexes.[37] The IFCT analysis provides valuable insights into the proportion of charge transfer between different fragments within the complexes, and the results are summarized in Tables S3 and S4 (ESI†). The charge transfer proportion from iridium to main ligand is 0.255, and that from main ligand to main ligand is 0.660 for **(2-pymICz)$_2$Ir(tmd)**, while the corresponding values are 0.287 and 0.641 for **(4-pymICz)$_2$Ir(tmd)**. These results suggest the emission components of both Ir(III) complexes are primarily attributed to the LC transition of cyclometalated ligand, with a secondary contribution from MLCT transition. Therefore, the design of the main ligand incorporating ICz is crucial for determining the photophysical and device properties of **(2-pymICz)$_2$Ir(tmd)** and **(4-pymICz)$_2$Ir(tmd)** complexes.

OLED performances

To evaluate the EL properties of the Ir(III) complexes, two devices, namely D1 and D2, were fabricated using **(2-pymICz)$_2$Ir(tmd)** and **(4-pymICz)$_2$Ir(tmd)** as emitters, respectively. The device structure employed was as follows: ITO (indium tin oxide)/HAT-CN (dipyrazino[2,3-*f*,2′,3′-*h*]quinoxaline-2,3,6,7,10,11-hexacarbonitrile, 5 nm)/TAPC (4,4′-cyclohexylidenebis[*N*,*N*-bis-(4-methylphenyl)aniline], 50 nm)/Ir(III) complex (7 wt%): 2,6DCzPPy (10 nm)/TmPyPB (1,3,5-tri(*m*-pyrid-3-yl-phenyl)benzene, 50 nm)/LiF (1 nm)/Al (100 nm). The device structure and chemical structures of materials used are shown in Scheme 2. HAT-CN and LiF served as hole and electron injection materials, while TAPC and TmPyPB acted as hole and electron transport material, respectively. The bipolar host material 2,6DCzPPy was used to minimize concentration quenching and TTA/TPA effects of Ir(III) complexes in the emissive layer, with an optimized 7 wt% doping concentrations. The characteristics of two devices are shown in Fig. 3, and the key characteristics are summarized in Table 2.

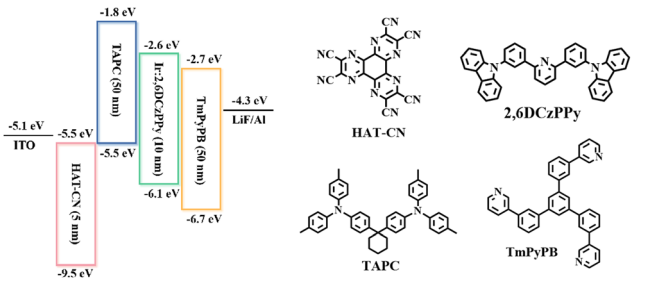

Scheme 2 Device energy diagram and molecule structures of materials used in each layer.

D1 and D2 exhibit green EL spectra with peaks at 511 and 519 nm and CIE coordinates of (0.26, 0.54) and (0.26, 0.62), respectively, which are consistent with the results observed in doped films. The EL spectra remained nearly identical across the applied voltage range of 5 to 12 V (Fig. S18, ESI†), indicating excellent spectral stability of the devices. The negligible emission from the host material in both devices indicates efficient energy transfer from the host material to the Ir(III) complexes in the emissive layer. In comparison to a previous device utilizing an Ir(III) complex based on ICz and pyridine with a FWHM of 33 nm,[10] D1 and D2 show slightly broadened EL spectra with FWHMs of 40 and 44 nm, respectively. However, the FWHM values still fall within a relatively narrow bandwidth.

Both devices display impressive OLED performances. D1, with **(2-pymICz)$_2$Ir(tmd)** as the emitter, exhibits a turn-on voltage ($V_{turn\text{-}on}$) of 3.3 V, a maximum luminance (L_{max}) above 40 000 cd m^{-2}, a maximum current efficiency ($\eta_{c,max}$) of 103.8 cd A^{-1}, a maximum power efficiency ($\eta_{p,max}$) of 98.8 lm W^{-1}, and an EQE$_{max}$ of 31.3%. D2, using **(4-pymICz)$_2$Ir(tmd)** as the emitter, displays slightly inferior characteristics with a L_{max} exceeding 40 000 cd m^{-2}, a $\eta_{c,max}$ of 95.3 cd A^{-1}, a $\eta_{p,max}$ of 93.6 lm W^{-1} and an EQE$_{max}$ of 26.0%. These differences could be attributed to the presence of a methyl group on the pyrimidine ring, leading to increased vibrations and transition categories, resulting in a broadened the spectrum and reduced device efficiency.

Moreover, both devices exhibit remarkably low efficiency roll-offs, with EQEs of 30.4% and 23.5% for D1 and D2, at a high brightness of 10 000 cd m^{-2}, implying efficiency roll-offs of 2.87% and 9.61%. The incorporation of the rigid ICz unit and nitrogen heterocycle pyrimidine units in the molecular structure plays a crucial role in mitigating self-quenching, achieving high PLQYs, and facilitating balanced carrier transport of Ir(III) complexes. These factors contribute to the low efficiency roll-offs observed in the devices. In comparison to our previous work on Ir(III) complexes containing main ligands based on ICz derivatives and pyridine,[10,16] the introduction of pyrimidine unit in main ligands not only tunes the photophysical and electrochemical properties but also evidently improves the OLED performances by enhancing the electron mobility and

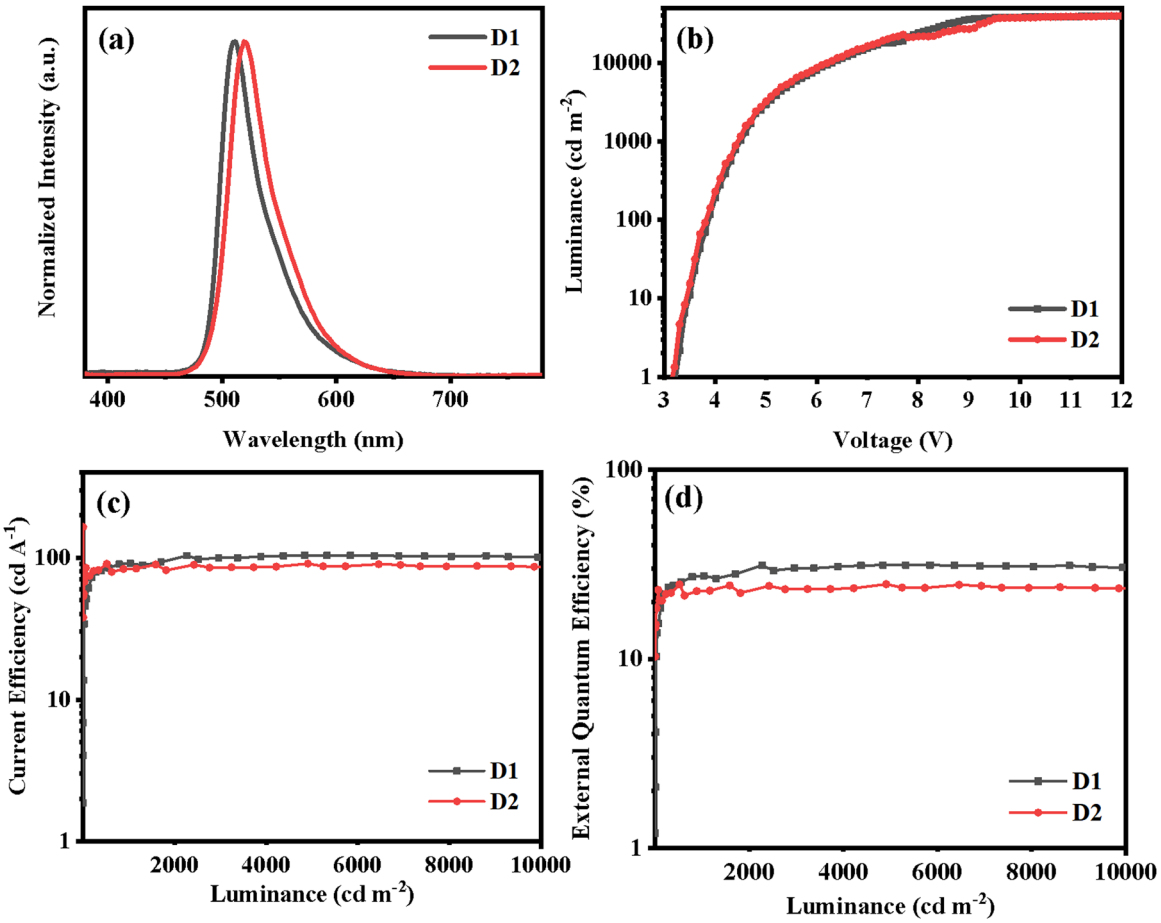

Fig. 3 EL performances of D1 and D2: (a) EL spectra at 6 V, (b) luminance–voltage (*L*–*V*) curves, (c) current efficiency–luminance (η_c–*L*) curves, and (d) external quantum efficiency–luminance (EQE–*L*) curves.

Table 2 Key EL data of D1 and D2

Device	$V_{turn\text{-}on}$[a] (V)	λ_{EL}[b] (nm)	FWHM[c] (nm)	L_{max}[d] (cd m^{-2})	$\eta_{c,max}$[e] (cd A^{-1})	$\eta_{c,10\,000}$[f] (cd A^{-1})	$\eta_{p,max}$[g] (lm W^{-1})	EQE_{max}[h] (%)	$EQE_{10\,000}$[i] (%)	CIE[j] (x, y)
D1	3.3	511	40	>40 000	103.8	100.9	98.8	31.3	30.4	(0.26, 0.54)
D2	3.2	519	44	>40 000	95.3	86.1	93.6	26.0	23.5	(0.26, 0.62)

[a] Turn-on voltage at 1 cd m^{-2}. [b] Electroluminescence peaks at 6 V. [c] Full width at half maximum. [d] Maximum luminance. [e] Maximum current efficiency. [f] Current efficiency at the brightness of 10 000 cd m^{-2}. [g] Maximum power efficiency. [h] Maximum external quantum efficiency calculated within the visible spectral region. [i] External quantum efficiency at the brightness of 10 000 cd m^{-2}. [j] CIE coordinates at an applied voltage of 6 V.

efficiency of Ir(III) complexes. These results suggest effectiveness of choosing the bipolar main ligands (**2-pymICz** and **4-pymICz**) can effectively balance the injection of charge carriers and reduce self-quenching, resulting in high efficiency and spectral stability of the devices.

Conclusions

In conclusion, two green Ir(III) complexes, **(2-pymICz)$_2$Ir(tmd)** and **(4-pymICz)$_2$Ir(tmd)**, were synthesized with high PLQYs and short lifetimes in solutions and doped films. The incorporation of the rigid ICz unit in the main ligands effectively constrains the intramolecular rotation and vibration of the Ir(III) complexes, resulting in narrow FWHMs. The OLEDs based on these Ir(III) complexes show good performances with narrow FWHMs of 40 and 44 nm. Notably, the device using **(2-pymICz)$_2$Ir(tmd)** exhibits superior performances, achieving an EQE_{max} of 31.3% with an extremely low efficiency roll-off of 2.87% at a high brightness of 10 000 cd m^{-2}. The introduction of the nitrogen heterocycle pyrimidine in the main ligands increases the electron transport ability of the complexes and improves the device efficiency with low efficiency roll-off. These findings underscore the potential of incorporating bulky and rigid ICz units to achieve narrow FWHMs and good device performances in Ir(III) complexes, thus demonstrating the promise of bipolar

main ligands in the development of efficient and stable Ir(III) complexes for OLED applications.

Conflicts of interest

There are no conflicts to declare.

Acknowledgements

This work was supported by the Guangdong Basic and Applied Basic Research Foundation (2020B1515120030) and the National Natural Science Foundation of China (21975119).

Notes and references

1 J. Kido, H. Hayase, K. Hongawa, K. Nagai and K. Okuyama, Bright redlight-emitting organic electroluminescent devices having a europium complex as an emitter, *Appl. Phys. Lett.*, 1994, **65**, 2124–2126.

2 R. C. Evans, P. Douglas and C. J. Winscom, Coordination complexes exhibiting room-temperature phosphorescence: Evaluation of their suitability as triplet emitters in organic light emitting diodes, *Coord. Chem. Rev.*, 2006, **250**, 2093–2126.

3 M. A. Baldo, D. F. O'Brien, Y. You, A. Shoustikov, S. Sibley, M. E. Thompson and S. R. Forrest, Highly efficient phosphorescent emission from organic electroluminescent devices, *Nature*, 1998, **395**, 151–154.

4 A. R. Bin Mohd Yusoff, A. J. Huckaba and M. K. Nazeeruddin, Phosphorescent neutral iridium(III) complexes for organic light-emitting diodes, *Top. Curr. Chem.*, 2017, **375**, 39.

5 K. S. Yook and J. Y. Lee, Organic materials for deep blue phosphorescent organic light-emitting diodes, *Adv. Mater.*, 2012, **24**, 3169–3190.

6 D. Ma, T. Tsuboi, Y. Qiu and L. Duan, Recent progress in ionic iridium(III) complexes for organic electronic devices, *Adv. Mater.*, 2017, **29**, 1603253.

7 (*a*) T.-Y. Li, J. Wu, Z.-G. Wu, Y.-X. Zheng, J.-L. Zuo and Y. Pan, *Coord. Chem. Rev.*, 2018, **374**, 55–92. 6; (*b*) Y. Zhou, R. Huang, J. Yan, Y. Li, H. Qiu, J. Yang and Y. Zheng, Synthesis and electroluminescence properties of two iridium(III) complexes with nitrogen heterocycle structures, *Chem. Res. Chin. Univ.*, 2022, **43**, 20210415.

8 W.-Y. Wong and C.-L. Ho, Heavy metal organometallic electrophosphors derived from multi-component chromophores, *Coord. Chem. Rev.*, 2009, **253**, 1709–1758.

9 W. Y. Wong, C. L. Ho, Z. Q. Gao, B. X. Mi, C. H. Chen, K. W. Cheah and Z. Lin, Multifunctional iridium complexes based on carbazole modules as highly efficient electrophosphors, *Angew. Chem., Int. Ed.*, 2006, **45**, 7800–7803.

10 X.-J. Liao, J.-J. Zhu, L. Yuan, Z.-P. Yan, X.-F. Luo, Y.-P. Zhang, J.-J. Lu and Y.-X. Zheng, Efficient organic light-emitting diodes based on iridium(III) complexes containing indolo[3,2,1-*jk*]carbazole derivatives with narrow emission bandwidths and low efficiency roll offs, *J. Mater. Chem. C*, 2021, **9**, 8226–8232.

11 G. Szafraniec-Gorol, A. Slodek, D. Zych, M. Vasylieva, M. Siwy, K. Sulowska, S. Maćkowski, I. Taydakov, D. Goriachiy and E. Schab-Balcerzak, Impact of the donor structure in new D–π–A systems based on indolo[3,2,1-*jk*]carbazoles on their thermal, electrochemical, optoelectronic and luminescence properties, *J. Mater. Chem. C*, 2021, **9**, 7351–7362.

12 P. Kautny, Z. Wu, J. Eichelter, E. Horkel, B. Stöger, J. Chen, D. Ma, J. Fröhlich and D. Lumpi, Indolo[3,2,1-*jk*]carbazole based planarized CBP derivatives as host materials for PhOLEDs with low efficiency roll-off, *Org. Electron.*, 2016, **34**, 237–245.

13 Y. Hiraga, R. Kuwahara and T. Hatta, Novel indolo[3,2,1-*jk*]-carbazole-based bipolar host material for highly efficient thermally activated delayed-fluorescence organic light-emitting diodes, *Tetrahedron*, 2021, **94**, 132317.

14 C. Luo, W. Bi, S. Deng, J. Zhang, S. Chen, B. Li, Q. Liu, H. Peng and J. Chu, Indolo[3,2,1-*jk*]carbazole derivatives-sensitized solar cells: effect of π-bridges on the performance of cells, *J. Phys. Chem. C*, 2014, **118**, 14211–14217.

15 T. Kader, G. Jin, M. Pletzer, D. Ma, J. Fröhlich, J. Chen and P. Kautny, Alkylated indolo[3,2,1-*jk*]carbazoles as new building blocks for solution processable organic electronics, *Org. Electron.*, 2021, **96**, 106215.

16 X.-J. Liao, J.-J. Zhu, L. Yuan, Z.-P. Yan, Z.-L. Tu, M.-X. Mao, J.-J. Lu, W.-W. Zhang and Y.-X. Zheng, Efficient organic light-emitting diodes with narrow emission bandwidths based on iridium(III) complexes with pyrido[3′,2′:4,5]pyrrolo[3,2,1-*jk*]carbazole unit, *Mater. Chem. Front.*, 2021, **5**, 6951–6959.

17 Y. C. Zhu, L. Zhou, H. Y. Li, Q. L. Xu, M. Y. Teng, Y. X. Zheng, J. L. Zuo, H. J. Zhang and X. Z. You, Highly efficient green and blue-green phosphorescent OLEDs based on iridium complexes with the tetraphenylimidodiphosphinate ligand, *Adv. Mater.*, 2011, **23**, 4041–4046.

18 E. Mondal, W.-Y. Hung, H.-C. Dai and K.-T. Wong, Fluorene-based asymmetric bipolar universal hosts for white organic light emitting devices, *Adv. Funct. Mater.*, 2013, **23**, 3096–3105.

19 J. Jin, W. Zhang, B. Wang, G. Mu, P. Xu, L. Wang, H. Huang, J. Chen and D. Ma, Construction of high T_g bipolar host materials with balanced electron–hole mobility based on 1,2,4-thiadiazole for phosphorescent organic light-emitting diodes, *Chem. Mater.*, 2014, **26**, 2388–2395.

20 X. Xu, X. Yang, Y. Wu, G. Zhou, C. Wu and W. Y. Wong, *tris*-Heteroleptic cyclometalated iridium(III) complexes with ambipolar or electron injection/transport features for highly efficient electrophosphorescent devices, *Chem. – Asian J.*, 2015, **10**, 252–262.

21 X. Xu, X. Yang, J. Dang, G. Zhou, Y. Wu, H. Li and W. Y. Wong, Trifunctional Ir^{III} ppy-type asymmetric phosphorescent emitters with ambipolar features for highly efficient electroluminescent devices, *Chem. Commun.*, 2014, **50**, 2473–2476.

22 P. Tao, W.-L. Li, J. Zhang, S. Guo, Q. Zhao, H. Wang, B. Wei, S.-J. Liu, X.-H. Zhou, Q. Yu, B.-S. Xu and W. Huang, Facile synthesis of highly efficient lepidine-based phosphorescent

iridium(III) complexes for yellow and white organic light-emitting diodes, *Adv. Funct. Mater.*, 2016, **26**, 881–894.

23 Y. Wang, Y. Lu, B. Gao, S. Wang, J. Ding, L. Wang, X. Jing and F. Wang, Self-host blue-emitting iridium dendrimer containing bipolar dendrons for nondoped electrophosphorescent devices with superior high-brightness performance, *ACS Appl. Mater. Interfaces*, 2016, **8**, 29600–29607.

24 Z. Yan, Y. Wang, J. Ding, Y. Wang and L. Wang, Highly efficient phosphorescent furo[3,2-*c*]pyridine based iridium complexes with tunable emission colors over the whole visible range, *ACS Appl. Mater. Interfaces*, 2018, **10**, 1888–1896.

25 J. B. Kim, S. H. Han, K. Yang, S. K. Kwon, J. J. Kim and Y. H. Kim, Highly efficient deep-blue phosphorescence from heptafluoropropyl-substituted iridium complexes, *Chem. Commun.*, 2015, **51**, 58–61.

26 S. Lee, S. O. Kim, H. Shin, H. J. Yun, K. Yang, S. K. Kwon, J. J. Kim and Y. H. Kim, Deep-blue phosphorescence from perfluoro carbonyl-substituted iridium complexes, *J. Am. Chem. Soc.*, 2013, **135**, 14321–14328.

27 J. Lv, Q. Liu, J. Tang, F. Perdih and K. Kranjc, A facile synthesis of indolo[3,2,1-*jk*]carbazoles via palladium-catalyzed intramolecular cyclization, *Tetrahedron Lett.*, 2012, **53**, 5248–5252.

28 N. Tian, D. Lenkeit, S. Pelz, D. Kourkoulos, D. Hertel, K. Meerholz and E. Holder, Screening structure–property correlations and device performance of Ir(III) complexes in multi-layer PhOLEDs, *Dalton Trans.*, 2011, **40**, 11629–11635.

29 X. F. Luo, Z. Z. Qu, H. B. Han, J. Su, Z. P. Yan, X. M. Zhang, J. J. Tong, Y. X. Zheng and J. L. Zuo, Carbazole-based iridium(III) complexes for electrophosphorescence with EQE of 32.2% and low efficiency roll-off, *Adv. Opt. Mater.*, 2020, **9**, 2001390.

30 J. Li, P. I. Djurovich, B. D. Alleyne, M. Yousufuddin, N. N. Ho, J. C. Thomas, J. C. Peters, R. Bau and M. E. Thompson, Synthetic control of excited-state properties in cyclometalated Ir(III) complexes using ancillary ligands, *Inorg. Chem.*, 2005, **44**, 1713–1727.

31 C.-L. Ho, B. Yao, B. Zhang, K.-L. Wong, W.-Y. Wong, Z. Xie, L. Wang and Z. Lin, Metallophosphors of iridium(III) containing borylated oligothiophenes with electroluminescence down to the near-infrared region, *J. Organomet. Chem.*, 2013, **730**, 144–155.

32 C. L. Yang, X. W. Zhang, H. You, L. Y. Zhu, L. Q. Chen, L. N. Zhu, Y. T. Tao, D. G. Ma, Z. G. Shuai and J. G. Qin, Tuning the energy level and photophysical and electroluminescent properties of heavy metal complexes by controlling the ligation of the metal with the carbon of the carbazole unit, *Adv. Funct. Mater.*, 2007, **17**, 651–661.

33 S. Bettington, M. Tavasli, M. R. Bryce, A. Beeby, H. Al-Attar and A. P. Monkman, Tris-Cyclometalated iridium(III) complexes of carbazole(fluorenyl)pyridine ligands: synthesis, redox and photophysical properties, and electrophosphorescent light-emitting diodes, *Chem. – Eur. J.*, 2007, **13**, 1423–1431.

34 Z. W. Liu, M. Guan, Z. Q. Bian, D. B. Nie, Z. L. Gong, Z. B. Li and C. H. Huang, Red phosphorescent iridium complex containing carbazole-functionalized β-diketonate for highly efficient nondoped organic light-emitting diodes, *Adv. Funct. Mater.*, 2006, **16**, 1441–1448.

35 Y. P. Zhang, X. Liang, X. F. Luo, S. Q. Song, S. Li, Y. Wang, Z.-P. Mao, W.-Y. Xu, Y.-X. Zheng, J.-L. Zuo and Y. Pan, Chiral spiro-axis induced blue thermally activated delayed fluorescence material for efficient circularly polarized OLEDs with low efficiency roll-off, *Angew. Chem., Int. Ed.*, 2021, **60**, 8435–8440.

36 X. Liang, F. Zhang, Z. P. Yan, Z. G. Wu, Y. Zheng, G. Cheng, Y. Wang, J. L. Zuo, Y. Pan and C. M. Che, Fast synthesis of iridium(III) complexes incorporating a bis(diphenylphorothioyl)amide ligand for efficient pure green OLEDs, *ACS Appl. Mater. Interfaces*, 2019, **11**, 7184–7191.

37 N. Natarajan, L.-X. Shi, H. Xiao, J.-Y. Wang, L.-Y. Zhang, X. Zhang and Z.-N. Chen, $PtAu_3$ cluster complexes with narrow-band emissions for solution-processed organic light emitting diodes, *J. Mater. Chem. C*, 2019, **7**, 2604–2614.